A Nonlinear Variational Multiscale Stabilized Method for Compressible Navier-Stokes Equations

Elaine Bernine(✉), Isaac P. Santos, and Lucia Catabriga

Federal University of Espírito Santo, Vitória, Brazil
elaine.bernine@edu.ufes.br, {isaac.santos,lucia.catabriga}@ufes.br

Abstract. In this work, we solve the compressible Navier-Stokes equations using a nonlinear variational multiscale finite element methodology. The numerical scheme relies on decomposing the problem into macro and micro scales, wherein an artificial viscosity operator is incorporated into both scales of the discretization. The magnitude of artificial viscosity is adjusted based on the stabilization parameter of the Consistent Approximate Upwind (CAU) method. To assess the performance of the method, we solve some problems for compressible Navier-Stokes equations. The numerical results indicate that the new method yields solutions similar to those obtained with the CAU method, however, with a lower computational cost.

Keywords: Finite element method · Compressible flow problems · Stabilized methods · Nonlinear Multiscale Viscosity

1 Introduction

The compressible Navier-Stokes equations are used to model fluid flows with variation in density, being applied to model fluid transport problems, such as effects caused by pollution of rivers, seas and soil, flow around airfoils of cars and planes, and propagation of smoke in fires and industrial chimneys. In general, the analytical solutions of these equations are difficult to obtain. To overcome this difficulty, we can resort to the use of numerical methods such as finite differences, finite volumes and finite elements. In this work, we focus on the discretization of equations via finite element approximation.

The standard Galerkin finite element methods may present numerical instabilities for convective-dominated problems, mainly due to the hyperbolic nature of the equations, which is the case of the compressible Navier-Stokes equations. In order to correct these oscillations, stabilized finite element methods have been developed for more than four decades. We highlight the Streamline Upwind Petrov-Galerkin (SUPG) [1,8] and Consistent Approximate Upwind (CAU) [4] stabilization methods to solve the Navier-Stokes equations.

This work has been supported in part by CAPES.

© The Author(s), under exclusive license to Springer Nature Switzerland AG 2024
O. Gervasi et al. (Eds.): ICCSA 2024 Workshops, LNCS 14815, pp. 251–267, 2024.
https://doi.org/10.1007/978-3-031-65154-0_16

The SUPG stabilization method is one of the most used for predominantly convective problems. This method is characterized by the addition of artificial viscosity only in the streamlines, obtaining good properties of stability and convergence, according to [8,13]. The SUPG stabilization matrix for the compressible Navier-Stokes equations, using conservative variables, was developed in [1,2] and later improved in [3]. In order to correct the oscillations of the SUPG method in the gradient elevation regions, the CAU non-linear stabilization method was developed in [10] for the advection-diffusion equation. This method inserts in a consistent way, besides the SUPG contribution, a discontinuity capturing operator that controls the derivatives in the direction of the gradient of the approximated solution. The CAU method was extended for compressible flows in [4], using entropy variables, and in [9], using conservative variables.

In the nineties, stabilized methods have been developed in the context of multiscale variational formulations, in order to obtain information contained at the micro scale. The multiscale variational stabilization (VMS) methods were introduced in [12] for the convection-diffusion equation and later [14] for compressible flow problems. These methods aim to decompose the problem of interest into two subproblems: one represented by the discretization of the domain used (macro scale - resolved scale) and the other by the smaller scales, sub-meshes (micro scale - unresolved scale). In [5,6] variations of the VMS method called Nonlinear Multiscale Viscosity (NMV) are developed, with the aim of numerically solving the system of compressible Euler Equations. The NMV methods add nonlinear artificial viscosity at both scales, defined by the YZβ method stabilization parameter [20].

In this work we redefine the NMV method for solving the compressible Navier-Stokes Equations. The artificial viscosity at both scales is defined by the discontinuity capture operator of the CAU method, that will be called NMVC. In order to validate the numerical implementation, we compared the results obtained between the NMVC and CAU methods in conservative variables for the Navier-Stokes equations. We emphasize that the temporal discretization was performed by the second-order predictor-multicorrector algorithm [6,11].

This work is organized as follows. In Sect. 2 the governing compressible Navier-Stokes equations are presented. In Sect. 3, the NMVC and CAU numerical formulations for the compressible Navier-Stokes equations are discussed. In Sect. 4 the predictor-multicorrect algorithm used as a time integration scheme is presented. Subsequently, in Sect. 5, numerical experiments on the compressible Navier-Stokes equation are presented in order to validate the numerical implementation of the NMVC method, in addition to showing the improvements in computational performance obtained. Finally, the conclusions of this work are presented.

2 Governing Equations

The compressible Navier-Stokes equations are obtained from a set of partial differential equations resulting from the laws of conservation of mass, motion

and energy. These equations are given by

$$\frac{\partial \rho}{\partial t} + \nabla \cdot (\rho \boldsymbol{u}) = \mathbf{0}, \quad \text{in } \Omega \times (0, t_f] \tag{1}$$

$$\frac{\partial \rho \boldsymbol{u}}{\partial t} + \nabla \cdot (\rho \boldsymbol{u} \otimes \boldsymbol{u}) + \nabla p - \nabla \cdot \boldsymbol{\sigma} = \boldsymbol{f}, \quad \text{in } \Omega \times (0, t_f] \tag{2}$$

$$\frac{\partial E_t}{\partial t} + \nabla \cdot [(E_t + p)\, \boldsymbol{u} - \boldsymbol{\tau} \boldsymbol{u} - \kappa \nabla T] = \mathbf{0}, \quad \text{in } \Omega \times (0, t_f] \tag{3}$$

where ρ, $\boldsymbol{u} = [u_1, u_2]^T$, $\boldsymbol{f}$, E_t, p, $\boldsymbol{\sigma}$, κ and T denote, respectively, density, velocity, source term, total energy, pressure, viscous stress tensor, thermal conductivity and temperature.

The viscous stress tensor $\boldsymbol{\tau}$ is defined as $\boldsymbol{\tau} = \lambda (\nabla \cdot \boldsymbol{u})\, I + 2\mu \varepsilon (\boldsymbol{u})$, where $\mu = \rho\nu$ is the first viscosity coefficient, $\lambda = -\frac{2\mu}{3}$ is the second viscosity coefficient (considering the ideal gas - Stokes hypothesis), ν is the kinematic viscosity, and $\varepsilon (\boldsymbol{u})$ is the strain tensor: $\varepsilon (\boldsymbol{u}) = \frac{1}{2} \left((\boldsymbol{\nabla u}) + (\boldsymbol{\nabla u})^T \right)$.

When considering the fluid as a perfect gas and based on the definitions presented in [17], we have $E_t = \rho \left(e_{in} + \frac{\|\boldsymbol{u}\|_2^2}{2} \right) = \rho E$, where $e_{in} = c_v T$ is the internal energy, $p = \rho R T$ is the pressure, $k = \gamma R \mu / (\gamma - 1) Pr$ is the thermal conductivity, c_v is the specific heat at constant volume, c_p is the specific heat at constant pressure, $\gamma = c_p / c_v$ is the adiabatic exponent, $R = c_p - c_v$ is the specific gas constant and Pr is the Prandtl number.

The compressible Navier-Stokes equations, represented by Eqs. (1), (2) e (3), can be rewritten in vector form with $x_1, x_2 \in \Omega \subset \mathbb{R}^2$ and $t \in (0, t_f]$ as

$$\frac{\partial U}{\partial t} + \frac{\partial F_i}{\partial x_i} - \frac{\partial G_i}{\partial x_i} = \mathbf{0}, \quad \text{with} \quad i = 1, 2, \tag{4}$$

where $U = [U_1, U_2, U_3, U_4]^T = [\rho, \rho u_1, \rho u_2, \rho E]^T$ is the vector of conservative variables, F_i is the Euler vector (advective transport terms) and G_i is the viscous flow vector (diffusive transport terms), for $i = 1, 2$, defined by

$$F_i = \begin{bmatrix} u_i \rho \\ u_i u_1 \rho + \delta_{1i} p \\ u_i u_2 \rho + \delta_{2i} p \\ u_i (\rho E + p) \end{bmatrix} \quad \text{and} \quad G_i = \begin{bmatrix} 0 \\ \boldsymbol{\tau}_{i1} \rho + \delta_{1i} p \\ \boldsymbol{\tau}_{i2} \rho + \delta_{2i} p \\ -q_i + \boldsymbol{\tau}_{ik} u_k \end{bmatrix}.$$

We emphasize that δ_{ij} represents the components of the identity tensor $I_{2\times 2}$ and $\boldsymbol{q} = -\kappa \boldsymbol{\nabla} T$ the components of the temperature flow vector. Furthermore, the Eq. (4) can be rewritten in the quasi-linear form,

$$\frac{\partial U}{\partial t} + A_i \frac{\partial U}{\partial x_i} - \frac{\partial}{\partial x_i} \left(K_{ij} \frac{\partial U}{\partial x_j} \right) = \mathbf{0}, \quad \text{in } \Omega \times (0, t_f], \quad \text{with} \quad i, j = 1, 2, \tag{5}$$

where $A_i = \frac{\partial F_i}{\partial U}$ are the Jacobian matrices and $G_i = K_{ij} \frac{\partial U}{\partial x_j}$, with $i = 1, 2$. Related to Eq. (5) we have an appropriate set of initial and Dirichlet boundary conditions assumed to be

$$BU = Z, \quad \text{in } \Gamma \times (0, t_f], \quad \text{and} \quad U_0(x) = U(x, 0),$$

with Γ being the boundary of domain Ω, B the general boundary operator, and Z and U_0 given functions.

3 Numerical Formulations

In this section we present two stabilized numerical formulations used to obtain the solutions of the compressible Navier-Stokes equations for a perfect gas: CAU method and the Nonlinear Multiscale Viscosity method considering the artificial viscosity defined by CAU parameter (NMVC).

Consider the partition $\mathcal{T}_h = \{K\}$ of the domain Ω into *nel* linear triangular elements, where h^e is the element length. Let $\mathcal{V}_h$ be the space of test functions defined by

$$\mathcal{V}_h = \{U_h \in \left[H^1(\Omega)\right]^4; \quad U_h|\Omega_e \in \left[\mathbb{P}^1(\Omega_e)\right]^4, \quad BU_h = Z \in \Gamma\}, \tag{6}$$

where $H^1(\Omega)$ is a Hilbert space of square integrable functions with square integrable (in the weak sense) first derivative, $\mathbb{P}^1(\Omega_e)$ is the set of linear polynomials defined in Ω_e, and Γ is the boundary of Ω with Dirichlet conditions.

3.1 The Consistent Approximate Apwind (CAU) Method

The CAU formulation of the compressible Navier-Stokes equations, presented in [4], consists of finding $U_h \in \mathcal{V}_h$, such that

$$\begin{aligned}
&\int_\Omega \left[W_h \left(\frac{\partial U_h}{\partial t} + A_i^h \frac{\partial U_h}{\partial x_i} \right) + \frac{\partial W_h}{\partial x_i} \left(K_{ij}^h \frac{\partial U_h}{\partial x_j} \right) \right] d\Omega + \\
&+ \sum_{e=1}^{nel} \int_{\Omega^e} \boldsymbol{\tau}_{\text{cau}} \left(A_i^h \frac{\partial W_h}{\partial x_i} \right) \cdot R(U_h) d\Omega_e + \\
&+ \sum_{e=1}^{nel} \int_{\Omega_e} \delta_{\text{cau}} \left(\frac{\partial W_h}{\partial x_i} \frac{\partial U_h}{\partial x_i} \right) d\Omega_e = \mathbf{0}, \quad \forall W_h \in \mathcal{V}_h,
\end{aligned} \tag{7}$$

with initial condition $U_0(x) = U_h(x, 0)$, where

$$R(U_h) = \frac{\partial U_h}{\partial t} + A_i^h \frac{\partial U_h}{\partial x_i}$$

is the local residue of the Eq. (5), $\boldsymbol{\tau}_{\text{cau}}$ is the stabilization parameter of the CAU method, defined as in [3] by $\boldsymbol{\tau}_{\text{cau}} = \max\{\mathbf{0}, \boldsymbol{\tau_t} + \zeta \cdot (\boldsymbol{\tau_a} - \boldsymbol{\tau_\delta} - \boldsymbol{\tau_d})\}$, with

$$\boldsymbol{\tau_t} = \frac{2}{3\,(1 + 2\alpha CFL)} \boldsymbol{\tau_a}, \qquad \boldsymbol{\tau_a} = \frac{h}{2\,(c + |\boldsymbol{u} \cdot \boldsymbol{\beta}|)} I, \qquad \boldsymbol{\tau_\delta} = \frac{\delta_{\text{cau}}}{(c + |\boldsymbol{u} \cdot \boldsymbol{\beta}|)^2} I$$

$$\text{and} \quad \boldsymbol{\tau_d} = \frac{\beta_1^2 \text{diag} K_{11} + \beta_2^2 \text{diag} K_{22}}{(c + |\boldsymbol{u} \cdot \boldsymbol{\beta}|)^2}.$$

Here, CFL is the Courant-Friedrichs-Lewy number, ζ is a weighting coefficient, and c is the acoustic velocity of the fluid, defined in [3] as

$$CFL = \frac{(c + |\boldsymbol{u} \cdot \boldsymbol{\beta}|)}{h}\Delta t, \quad \zeta = \frac{2\alpha CFL}{1 + 2\alpha CFL}, \quad c^2 = \gamma(\gamma - 1)\left(E - \frac{\|\boldsymbol{u}\|^2}{2}\right),$$

where $h^e = \sqrt{2A^e}$ is the element length, A^e is the area of the element Ω_e, and $\boldsymbol{\beta}$ is given by the expression

$$\boldsymbol{\beta} = \frac{\boldsymbol{\nabla}\|\boldsymbol{U}\|_2^2}{\left\|\boldsymbol{\nabla}\|\boldsymbol{U}\|_2^2\right\|_2}.$$

Finally, δ_{cau} is the discontinuity capturing parameter of the CAU method in conservative variables, defined in [9] as

$$\delta_{\text{cau}} = \begin{cases} \frac{\|R(U^h)\|}{\|\boldsymbol{\nabla}_\xi U^h\|_{\tilde{A}_0^{-1}}}, & \text{if } |\boldsymbol{\nabla} U^h|_{\tilde{A}_0^{-1}} > tol_\delta, \\ 0, & \text{otherwise,} \end{cases} \tag{8}$$

where

$$\left\|\boldsymbol{\nabla}_\xi U^h\right\|_{\tilde{A}_0^{-1}} = \left\|\frac{\partial x}{\partial \xi}\frac{\partial U^h}{\partial x} + \frac{\partial y}{\partial \xi}\frac{\partial U^h}{\partial y}\right\|_{\tilde{A}_0^{-1}} + \left\|\frac{\partial x}{\partial \eta}\frac{\partial U^h}{\partial x} + \frac{\partial y}{\partial \eta}\frac{\partial U^h}{\partial y}\right\|_{\tilde{A}_0^{-1}},$$

and tol_δ is a small positive real number used to prevent division by zero. In this work we use $tol_\delta = 10^{-8}$. The norm $\|\cdot\|_{\tilde{A}_0^{-1}}$ is defined as $\|\boldsymbol{w}\|_{\tilde{A}_0^{-1}} = \left(\boldsymbol{w}^T \tilde{A}_0^{-1} \boldsymbol{w}\right)^{1/2}$, for all vector $\boldsymbol{w}$ and $\tilde{A}_0^{-1}$ is the inverse of the Reimannian matrix tensor defined in [19].

The variational formulation described in Eq. (7) results in the global system of algebraic differential equations given by

$$M\dot{U}_h + KU_h = \mathbf{0}, \tag{9}$$

with U_h being the unknowns derived from each element Ω_e, $\dot{U}_h$ being their derivatives with respect to time, and M and K are matrices derived from Eq. (7).

3.2 The Nonlinear Multiscale Variational (NMVC) Method

Let $\mathcal{V}_E$ be the enriched space defined by the direct sum between the space of macro scales, $\mathcal{V}_h$, defined in Eq. (6), and space of micro scales, $\mathcal{V}_b$, spanned by bubble functions, $\mathcal{V}_E = \mathcal{V}_h \oplus \mathcal{V}_b$, where

$$\mathcal{V}_b = \{U_b \in \left[H^1(\Omega)\right]^4; \quad U_b|\Omega_e \in [\text{span}(\phi_B)]^4, \quad \forall \Omega_e \in \mathcal{T}_h\}.$$

The bubble function ϕ_B is defined in Ω_e as $\phi_B = 27N_1^e N_2^e N_3^e$, where $N_j^e = N_j^e(x, y)$ are the (local) basis function of space V_h.

The nonlinear multiscale variational (NMVC) method for the compressible Navier-Stokes equations consists of finding $U_E = U_h + U_b \in \mathcal{V}_E$, with $U_h \in \mathcal{V}_h$ and $U_b \in \mathcal{V}_b$, such that

$$\int_\Omega \left[W_E \cdot \left(\frac{\partial U_E}{\partial t} + A_i^h \frac{\partial U_E}{\partial x_i} \right) + \frac{\partial W_E}{\partial x_i} \cdot \left(K_{ij}^h \frac{\partial U_E}{\partial x_j} \right) \right] d\Omega + \\ + \sum_{e=1}^{nel} \int_{\Omega_e} \delta_{\text{cau}}(U_h) \left(\frac{\partial W_E}{\partial x_i} \cdot \frac{\partial U_E}{\partial x_i} \right) d\Omega = \mathbf{0}, \quad \forall W_E \in \mathcal{V}_E, \tag{10}$$

where $W_E = W_h + W_b \in \mathcal{V}_E$, whith $W_h \in \mathcal{V}_h$ and $W_b \in \mathcal{V}_b$, and $\delta_{\text{cau}}(U_h)$ is the discontinuity capturing parameter of the CAU method, defined in Eq. (8).

The variational formulation presented in the system (10) can be divided into two systems that concern the macro and micro scale, respectively. Thus, for the space of macro scales, we will have

$$\int_\Omega \left[W_h \cdot \left(\frac{\partial U_h}{\partial t} + A_i^h \frac{\partial U_h}{\partial x_i} \right) + W_h \cdot \left(\frac{\partial U_b}{\partial t} + A_i^h \frac{\partial U_b}{\partial x_i} \right) \right] d\Omega + \\ + \int_\Omega \frac{\partial W_h}{\partial x_i} \cdot \left(K_{ij}^h \frac{\partial U_h}{\partial x_j} \right) d\Omega + \\ + \sum_{e=1}^{nel} \int_{\Omega_e} \delta_{\text{cau}}(U_h) \left(\frac{\partial W_h}{\partial x_i} \cdot \frac{\partial U_h}{\partial x_i} \right) d\Omega = \mathbf{0}, \quad \forall W_h \in \mathcal{V}_h. \tag{11}$$

For the space of micro scales, we have

$$\int_\Omega \left[W_b \cdot \left(\frac{\partial U_h}{\partial t} + A_i^h \frac{\partial U_h}{\partial x_i} \right) + W_b \cdot \left(\frac{\partial U_b}{\partial t} + A_i^h \frac{\partial U_b}{\partial x_i} \right) \right] d\Omega + \\ + \int_\Omega \frac{\partial W_b}{\partial x_i} \cdot \left(K_{ij}^h \frac{\partial U_b}{\partial x_j} \right) d\Omega + \\ + \sum_{e=1}^{nel} \int_{\Omega_e} \delta_{\text{cau}}(U_h) \left(\frac{\partial W_b}{\partial x_i} \cdot \frac{\partial U_b}{\partial x_i} \right) d\Omega = \mathbf{0}, \quad \forall W_b \in \mathcal{V}_b. \tag{12}$$

When finite element approximations are used in the systems of Eqs. (11) and (12), considering homogeneous Dirichlet boundary conditions (i.e., $Z = \mathbf{0}$ in Γ), we obtain the following system of differential algebraic equations

$$\begin{bmatrix} M_{hh} & M_{hb} \\ M_{bh} & M_{bb} \end{bmatrix} \begin{bmatrix} \dot{U}_h \\ \dot{U}_b \end{bmatrix} + \begin{bmatrix} K_{hh} & K_{hb} \\ K_{bh} & K_{bb} \end{bmatrix} \begin{bmatrix} U_h \\ U_b \end{bmatrix} = \begin{bmatrix} \mathbf{0}_h \\ \mathbf{0}_b \end{bmatrix}, \tag{13}$$

with U_h and U_b being the unknowns derived from each element Ω_e, and $\dot{U}_h$ and $\dot{U}_b$ being their derivatives with respect to time. All matrices are defined based on Eqs. (11) and (12).

4 Time Integration Schemes

In order to solve the given system of differential equations by Eq. (9) we use the well known time integration scheme given by the predictor-multicorrector

method based on implicit methods, as described in [11]. To solve the system of differential equations obtained by the NMVC method (Eq. (13)) we adapted the predictor-multicorrector method considering a static condensation, as described in Algorithm 1. In both systems, we consider $\alpha = 0.5$ in all experiments, thus obtaining a second order approximation for the time derivative of U_h and U_b, with U_h^n and U_b^n being the solution of the macro and micro scales of U in step of time n and Δt the time step.

Algorithm 1. NMVC Predictor-multicorrector algorithm

Input: U_h^n, $\dot{U}_h^n$, U_b^n and $\dot{U}_b^n$
$t = 0$
Predictor phase:
$t = t + \Delta t$
$U_h^{n+1,0} = U_h^n + (1-\alpha)\,\Delta t \dot{U}_h^n$
$\dot{U}_h^{n+1,0} = 0$
$U_b^{n+1,0} = U_b^n + (1-\alpha)\,\Delta t \dot{U}_b^n$
$\dot{U}_b^{n+1,0} = 0$
$i = 0$
Multicorrector phase:
Calculate residue:
$R_1^{n+1,i} = -\left(M_{hh}\dot{U}_h^{n+1,i} + M_{hb}\dot{U}_b^{n+1,i}\right) - \left(K_{hh}U_h^{n+1,i} + K_{hb}U_b^{n+1,i}\right)$
$R_2^{n+1,i} = -\left(M_{bh}\dot{U}_h^{n+1,i} + M_{bb}\dot{U}_b^{n+1,i}\right) - \left(K_{bh}U_h^{n+1,i} + K_{bb}U_b^{n+1,i}\right)$
Solve:
$M^*\dot{U}_h = F^*$,
with $M^* = M_1 - N_1 N_2^{-1} M_2$ and $F^* = R_1 - N_1 N_2^{-1} R_2$,
where $M_1 = M_{hh} + \alpha\Delta t K_{hh}$, $M_2 = M_{bh} + \alpha\Delta t K_{bh}$,
$N_1 = M_{hb} + \alpha\Delta t K_{hb}$ and $N_2 = M_{bb} + \alpha\Delta t K_{bb}$
Corrector:
$U_h^{n+1,i+1} = U_h^{n,i} + (1-\alpha)\,\Delta t \dot{U}_h^{n+1,i+1}$
$\dot{U}_h^{n+1,i+1} = \dot{U}_h^{n+1,i} + \Delta\dot{U}_h^{n+1,i+1}$
$U_b^{n+1,i+1} = U_b^{n,i} + (1-\alpha)\,\Delta t \dot{U}_b^{n+1,i+1}$
$\dot{U}_b^{n+1,i+1} = \dot{U}_b^{n+1,i} + \Delta\dot{U}_b^{n+1,i+1}$
with $\Delta\dot{U}_b^{n+1,i+1} = N_2^{-1}\left(R_2^{n+1,i} - M_2\Delta\dot{U}_b^{n+1,i+1}\right)$

5 Numerical Experiments

In this section, we present four numerical experiments, in order to compare the results obtained for the CAU and NMVC methods, described previously. The code was built in *C* Language based on the finite element library called FEM_CODES[1] - under development by the UFES Computational Optimization and Modeling Laboratory.

[1] Available in https://github.com/mod-comp-ufes/FEM_CODES.

In order to validate the numerical implementation, we present the oblique and reflected shock problems that use the compressible Euler equation, and the Carter's flat plate and compression corner problems that use the compressible Navier-Stokes equations. In all experiments, compressible gases are considered with specific heat at constant volume $c_v = 717.5$, specific heat at constant pressure $c_p = 1004.5$, gas constant $R = 287$, adiabatic exponent $\gamma = 1.4$ and Prandtl number $Pr = 0.72$. To carry out the experiments, we use the GMRES solver with a maximum number of cycles 100, 30 vectors in Krylov basis, solver tolerance 10^{-5}, 3 fixed nonlinear corrections, step-time 10^{-2}, BlockDiag preconditioner, element-by-element matrix-vector product and triangular meshes. The numerical experiments were carried out on a machine with an Intel®Core^{TM}i5-1035G1 CPU @ 1.00GHz processor, memory 8 GB of RAM and Ubuntu 20.04.5 LTS as operating system.

5.1 Oblique Shock Problem

The oblique shock problem, described in [7,19], consists of supersonic flow ($M = 2.0$) over a wedge located in the lower part of the domain $\Omega = [0.0, 1.0] \times [0.0, 1.0]$. The fluid enters at an angle of $-10°$ with respect to the wedge and the oblique shock occurs in the lower left corner with an angle of 29.3°, as described in Fig. 1.

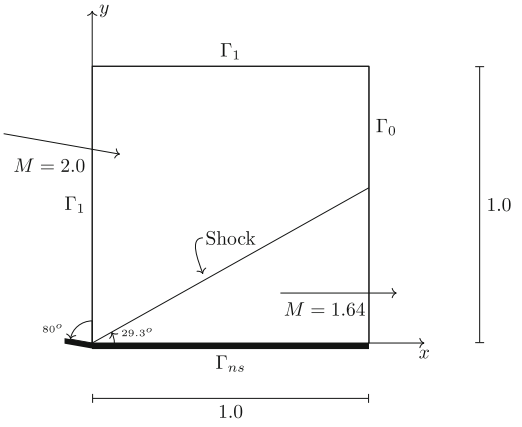


Fig. 1. Oblique shock problem description.

The specified boundary conditions are: in Γ_1 all variables are prescribed as $\{U_1, U_2, U_3, U_4\} = \{1.0, \cos 10°, -\sin 10°, 0.94643\}$; in Γ_{ns} the normal speed to the wall is zero, i.e., $U_3 = 0$; in Γ_0 no boundary conditions are prescribed.

The numerical results were analyzed at the time instant $t = 3.0\,\mathrm{s}$ with an unstructured mesh with 474 nodes and 874 triangular elements. The Fig. 2 shows the density profile of the oblique shock problem along $x = 0.9$ comparing the

NMVC, CAU methods and their exact solution. Note that the results obtained by the NMVC and CAU methods are similar.

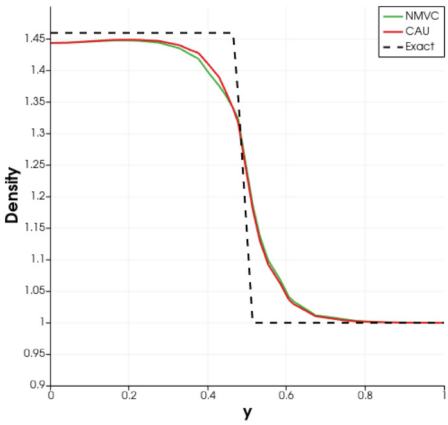


Fig. 2. Density profile along $x = 0.9$ of the oblique shock problem.

Figures 3a and 3b show the numerical results obtained by the NMVC method for the density and pressure, respectively, of the oblique shock problem. The numerical results can be compared with those presented in [5,9] with the CAU stabilization method.

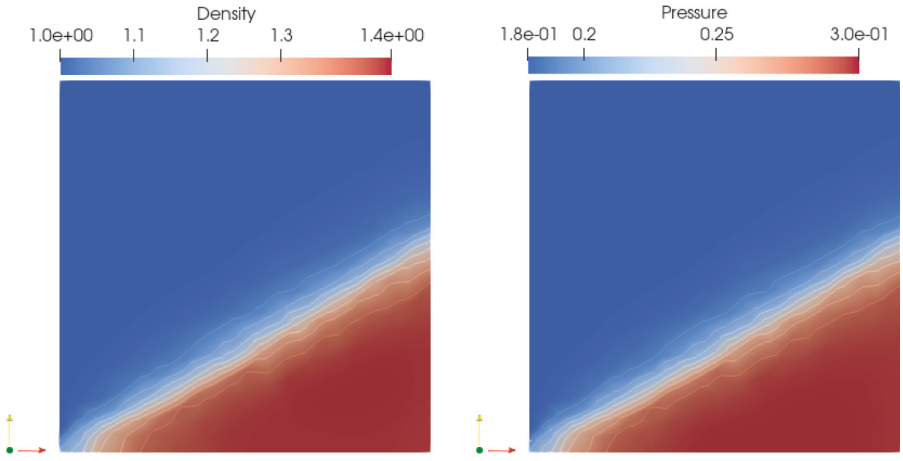
Table 1 presents computational performance data between the NMVC and CAU methods with regard to the number of GMRES iterations and the CPU time spent. The NMVC method obtained the shortest time and the fewest number of iterations, being 19.56% faster than the CAU method.

Table 1. Computational performance of the oblique shock problem.

Methods	GMRES Iterations	CPU Time (s)
NMVC	06126	3.948
CAU	10325	4.908

5.2 Reflected Shock Problem

The reflected shock as describe in [19], is a two-dimensional stationary problem composed of three flow regions separated by an oblique shock and its reflection along the bottom wall. The computational domain is given by $\Omega = [0.0, 4.1] \times [0.0, 1.0]$, as shown in Fig. 4.



(a) Density. (b) Pressure.

Fig. 3. Numerical results of oblique shock problem.

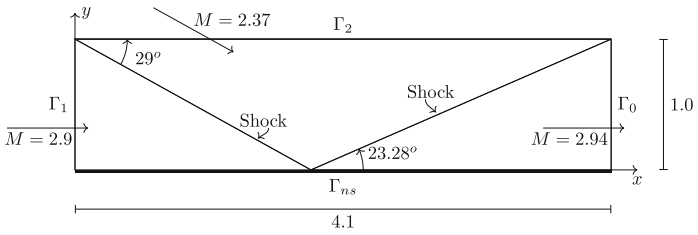


Fig. 4. Reflected shock problem description.

The prescribed boundary conditions are: in Γ_1 all variables are prescribed as $\{U_1, U_2, U_3, U_4\} = \{1.0, 2.9, 0.0, 5.990715\}$; in Γ_2 all variables are prescribed as $\{U_1, U_2, U_3, U_4\} = \{1.7, 4.452878, -0.860744, 9.870181\}$; in Γ_{ns} the normal speed to the wall is zero, i.e., $U_3 = 0$; in Γ_0 no boundary conditions are prescribed.

The results of the reflected shock problem were analyzed at time $t = 3.0$s with an unstructured mesh with 1404 nodes and 2646 triangular elements. The Fig. 5 presents the density profile of the reflected shock problem along $y = 0.25$ comparing the results obtained from the NMVC and CAU methods, and the exact solution of the problem. From the presented results of the density profile, we can verify the similarity between the NMVC and CAU methods.

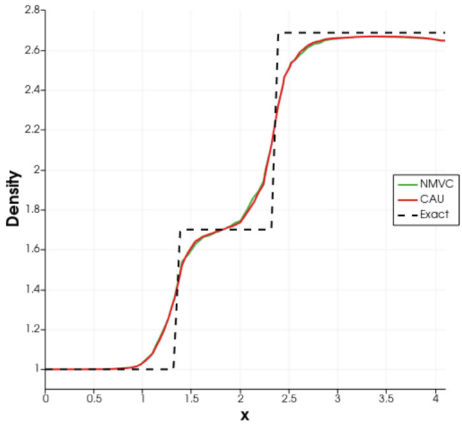
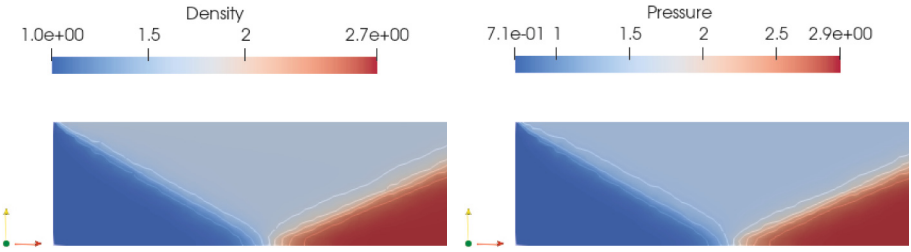


Fig. 5. Density profile along $y = 0.25$ of the reflected shock problem.

Figures 6a and 6b present the numerical results obtained by the NMVC method for the density and pressure, respectively, of the reflected shock problem. The computational performance data of the NMVC and CAU methods for the reflected shock problem are presented in Table 2. Note that the number of GMRES iterations and the CPU time of the NMVC method are better compared to the CAU method, leading the NMVC method to be 8.34% faster in this problem.

Table 2. Computational performance of the reflected shock problem.

Methods	GMRES Iterations	CPU Time (s)
NMVC	7515	13.136
CAU	9238	14.331



(a) Density. (b) Pressure.

Fig. 6. Numerical results of reflected shock problem.

5.3 Carter's Flat Plate Problem

The Carter's flat plate problem has a two-dimensional domain $\Omega = [-0.2, 1.2] \times [0.0, 0.8]$, Reynolds number $Re = 1000$ and Mach number $M = 3.0$. The flat plate is set in the range $0.0 \leq x \leq 1.2$, as shown in Fig. 7. We emphasize that thermal conductivity was defined as $\kappa = 1.395138$, as described in [16,21]. The viscosity is related to temperature through the equation $\mu = (0.0906T^{1.5})/(T + 0.0001406)$.

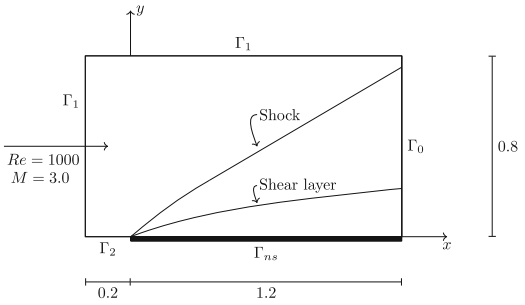


Fig. 7. Carter's flat plate problem description.

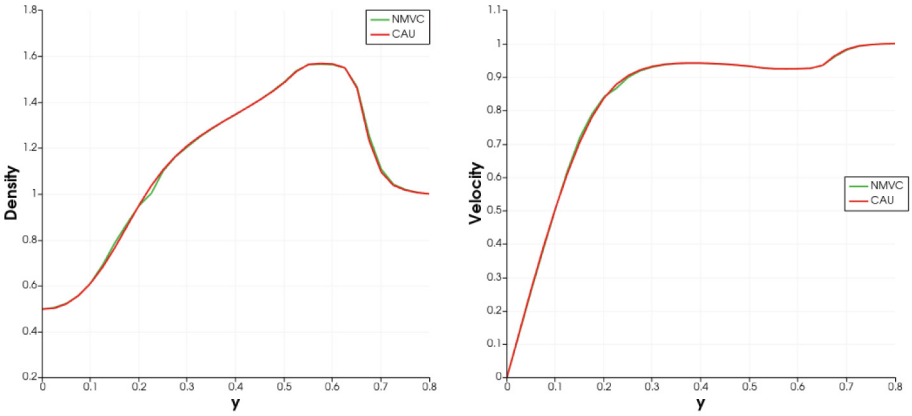
The specified boundary conditions are: in Γ_1 all variables are prescribed as $\{U_1, U_2, U_3, U_4\} = \{1.0, 1.0, 0.0, 0.698675\}$ and reference temperature $T_0 = 2.769 \times 10^{-4}$; in Γ_2 homogeneous Neumann boundary conditions are prescribed and $U_3 = 0$; in Γ_{ns} no-slip conditions are imposed $u_1 = u_2 = 0$ and stagnation temperature $T_{\text{stag}} = 7.7532 \times 10^{-4}$; in Γ_0 no boundary conditions are prescribed.

The numerical solutions were obtained at time $t = 3.5$s with a structured mesh with 1881 nodes and 3584 elements. Figures 8a and 8b present the density and velocity profile of the Carter's flat plate problem over $x = 1.0$ for the NMVC and CAU methods. Those numerical results can be compared with those presented in [15,16,18] with spectral elements and use SUPG stabilization method with the YZβ capture operator. The solutions obtained are similar, showing the effectiveness of implementing the NMVC method with the artificial viscosity operator given by the CAU discontinuity capture operator.

Figures 9a, 9b, 9c and 9d present the results of density, Mach number, pressure and temperature, respectively, from the Carter's flat plate problem. The contour lines can be compared with those presented in [4], where it uses the CAU stabilization method.

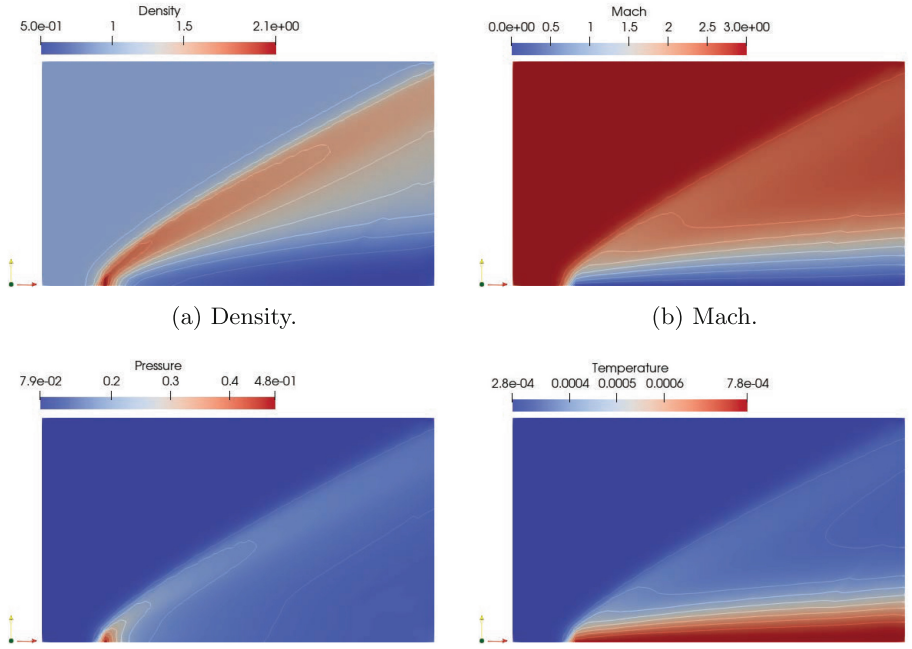
The friction coefficient of the Carter's flat plate problem is presented in Fig. 10, comparing the results obtained with the NMVC and CAU methods, and the modified Blasius solution [1]. Note that the solutions obtained by the NMVC and CAU methods are equivalent and close to the value of the modified Blasius solution.

The results of the computational performance of the NMVC and CAU methods for the Carter's flat plate problem are presented in Fig. 3. With the data



(a) Density. (b) Velocity.

Fig. 8. Profile along $x = 1.0$ of the Carter's flat plate.



(a) Density. (b) Mach.

(c) Pressure. (d) Temperature.

Fig. 9. Numerical results of Carter's flat plate.

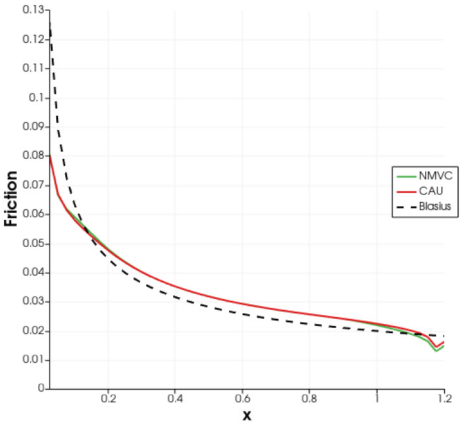


Fig. 10. Friction coefficient of Carter's flat plate problem.

we can verify the best performance of the NMVC method, obtaining the lowest number of iterations of the GMRES method and the lowest CPU time. In this way, we can see that the NMVC method is 24.86% faster than the CAU method for the Carter's flat plate problem (Table 3).

Table 3. Computational performance of the Carter's flat plate problem.

Methods	GMRES Iterations	CPU Time (s)
NMVC	07369	19.373
CAU	12475	24.481

5.4 Compression Corner Problem

The compression corner problem has a two-dimensional domain given by a rectangular part $[-0.2, 1.0] \times [0.0, 0.575]$ and by a part with slope of $10°$ given by $[1.0, 1.8] \times [0.8 \tan 10°, 0.575 + 0.8 \tan 10°]$, as shown in Fig. 11. According to [18,21], the flat plate is located after $x = 0.0$, and the following are considered at the input: Reynolds number $Re = 16800$, Mach number $M = 3.0$ and conductivity thermal $\kappa = 1.395138$. Viscosity is related to temperature through the equation $\mu = (0.00539T^{1.5})/(T + 0.0001406)$.

The specified boundary conditions are: in Γ_1 all variables are prescribed as $\{U_1, U_2, U_3, U_4\} = \{1.0, 1.0, 0.0, 0.698675\}$ and reference temperature $T_0 = 2.769 \times 10^{-4}$; in Γ_2 homogeneous Neumann boundary conditions are prescribed and $U_3 = 0$; in Γ_{ns} no-slip conditions are imposed $u_1 = u_2 = 0$ and stagnation temperature $T_{\text{stag}} = 7.7532 \times 10^{-4}$; in Γ_0 no boundary conditions are prescribed.

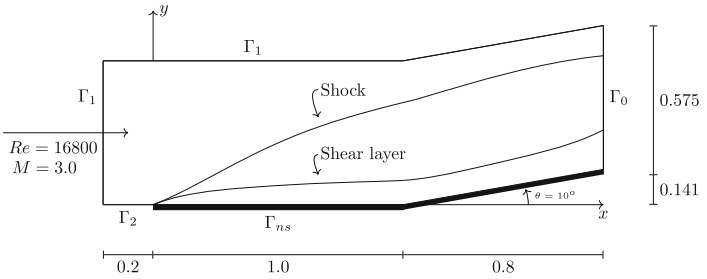
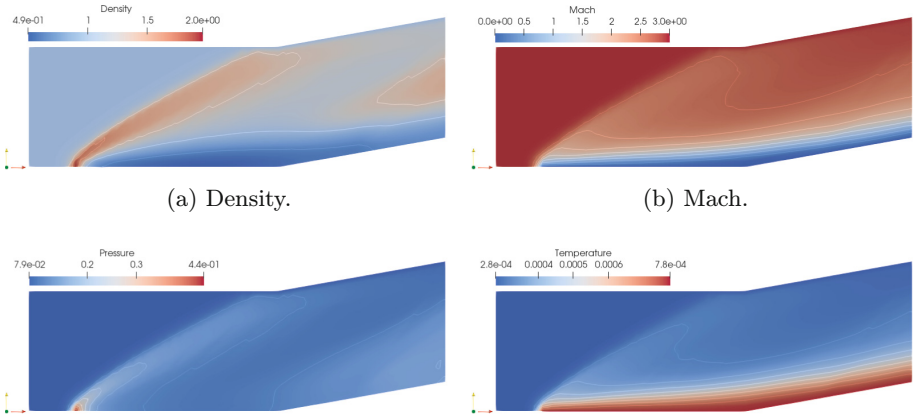


Fig. 11. Compression corner problem description.

The Figs. 12a, 12b, 12c and 12d present the density, Mach number, pressure and temperature for the compression corner problem, respectively. The results presented can be compared with those obtained in [21] using the SUPG stabilization method with the YZβ capture operator and [15] with a method based on the finite calculus (FIC). We emphasize that the solutions were obtained at the time instant $t = 3.0$s with a structured mesh with 1944 nodes and 3680 elements.



(a) Density. (b) Mach.

(c) Pressure. (d) Temperature.

Fig. 12. Numerical results of compression corner problem.

The results of the computational performance of the NMVC and CAU methods for the compression corner problem are presented in Table 4. With the tabulated data we can see that the NMVC method has better performance compared to the CAU method, with the NMVC method being 24.16% faster for the compression corner problem.

Table 4. Computational performance of the compression corner problem.

Methods	GMRES Iterations	CPU Time (s)
NMVC	07628	18.426
CAU	13274	24.299

6 Conclusions

In this work, we present the NMVC method of multiscale variational stabilization with nonlinear artificial viscosity for the compressible Navier-Stokes equations with the bubble functions scenario. This method adds artificial viscosity in the two discretization scales of the problem, which is defined by the discontinuity capture operator of the CAU method.

The NMVC and CAU methods were used to obtain the numerical solution of four problems comprising the Euler and compressible Navier-Stokes equations. The results obtained from the methods were compared and validated the implementation of the NMVC method, since the solutions obtained by the methods are similar. We also highlight the better computational performance obtained by the NMVC method, leading to faster solutions from 8 to 24%.

References

1. Aliabadi, S.K., Ray, S.E., Tezduyar, T.E.: SUPG finite element computation of viscous compressible flows based on the conservation and entropy variables formulations. Comput. Mech. **11**, 300–312. Springer (1993). https://doi.org/10.1007/BF00350089
2. Aliabadi, S.K., Tezduyar, T.E.: Space-time finite element computation of compressible flows involving moving boundaries and interfaces. Comput. Methods Appl. Mech. Eng. **107**(1-2), 209–223 (1993). https://doi.org/10.1016/0045-7825(93)90176-X
3. Aliabadi, S.K., Tezduyar, T.E.: Parallel fluid dynamics computations in aerospace applications. Int. J. Numer. Methods Fluids **21**(10), 783–805 (1995). https://doi.org/10.1002/fld.1650211003
4. Almeida, R.C., Galeão, A.C.: An adaptive Petrov-Galerkin formulation for the compressible Euler and Navier-Stokes equations. Comput. Methods Appl. Mech. Eng. **129**(1-2), 157–176 (1996). https://doi.org/10.1016/0045-7825(95)00858-6
5. Bento, S.S., de Lima, L.M., Sedano, R.Z., Catabriga, L., Santos, I.P.: A nonlinear multiscale viscosity method to solve compressible flow problems. In: Gervasi, O., et al. (eds.) ICCSA 2016. LNCS, vol. 9786, pp. 3–17. Springer, Cham (2016). https://doi.org/10.1007/978-3-319-42085-1_1
6. Bento, S.S., Barbosa, P.W., Santos, I.P., de Lima, L.M., Catabriga, L.: A nonlinear finite element formulation based on multiscale approach to solve compressible Euler equations. In: Gervasi, O., et al. (eds.) ICCSA 2017. LNCS, vol. 10409, pp. 735–743. Springer, Cham (2017). https://doi.org/10.1007/978-3-319-62407-5_55
7. Bento, S.S.: Nonlinear multiscale viscosity methods and time integration schemes for solving compressible Euler equations. DSc Thesis, Universidade Federal do Espírito Santo, Vitória - ES, Brasil (2018)

8. Brooks, A.N., Hughes, J.R.: Streamline upwind/Petrov-Galerkin formulations for convection dominated flows with particular emphasis on the incompressible Navier-Stokes equations. Comput. Methods Appl. Mech. Eng. **32**(1-3), 199–259 (1982). https://doi.org/10.1016/0045-7825(82)90071-8
9. Catabriga, L., Coutinho, A.L.G.A.: Implicit SUPG solution of Euler equations using edge-based data structures. Comput. Methods Appl. Mech. Eng. **191**, 3477-3490 (2002). https://doi.org/10.1016/S0045-7825(02)00285-2
10. Galeão, A.C., Do Carmo, E.G.D.,: A consistent approximate upwind Petrov-Galerkin method for convection-dominated problems. Comput. Methods Appl. Mech. Eng. **68**(1), 83–95 (1988). https://doi.org/10.1016/0045-7825(88)90108-9
11. Hughes, T.J.R., Tezduyar, T.E.: Finite element methods for first-order hyperbolic systems with particular emphasis on the compressible Euler equations. Comput. Methods Appl. Mech. Eng. **45**, 217–284 (1984). https://doi.org/10.1016/0045-7825(84)90157-9
12. Hughes, T.J.R.: Multiscale phenomena: Green's functions, the Dirichlet-to-Neumann formulation, subgrid scale models, bubbles and the origins of stabilized methods. Elsevier. Comput. Methods Appl. Mech. Eng. **127**(1-4), 387–401 (1995). https://doi.org/10.1016/0045-7825(95)00844-9
13. Knobloch, P.: Improvements of the Mizukami–Hughes method for convection–diffusion equations. Comput. Methods Appl. Mech. Eng. **196**(1-3), 579–594 (2006). https://doi.org/10.1016/j.cma.2006.06.004
14. Koobus, B., Farhat, C.: A variational multiscale method for the large eddy simulation of compressible turbulent flows on unstructured meshes-application to vortex shedding. Comput. Methods Appl. Mech. Eng. **193**(15-16), 1367–1383 (2004). https://doi.org/10.1016/j.cma.2003.12.028
15. Kouhi, M., Oñate, E.: An implicit stabilized finite element method for the compressible Navier-Stokes equations using finite calculus. Comput. Mech. **56**, 113-129 (2015). https://doi.org/10.1007/s00466-015-1161-2
16. Parada, S., Codina, R., Baiges, J.: A VMS-based fractional step technique for the compressible Navier-Stokes equations using conservative variables. J. Comput. Phys. **459**, 111–137 (2022). https://doi.org/10.1016/j.jcp.2022.111137
17. Quarteroni, A.: Numerical models for differential problems, 2nd edn. Springer, Milano (2009). https://doi.org/10.1007/978-88-470-5522-3
18. Ranjan, R., Catabriga, L., Yusheng, F.: High-Order Spectral/hp-Based Solver for Compressible Navier-Stokes Equations. AIAA J. **60**(5), 2972–2986 (2022). https://doi.org/10.2514/1.J060704
19. Shakib, F.T., Hughes, J.R., Johan, Z.: A new finite element formulation for computational fluid dynamics: X. The compressible Euler and Navier-Stokes equations. Comput. Methods Appl. Mech. Eng. **89**(1-3), 141–219 (1991). https://doi.org/10.1016/0045-7825(91)90041-4
20. Tezduyar, T.E., Senga, M.: Stabilization and shock-capturing parameters in SUPG formulation of compressible flows. Comput. Methods Appl. Mech. Eng. **195**, 1621–1632 (2006). https://doi.org/10.1016/j.cma.2005.05.032
21. Toro, J.B.: Implementation of finite element solvers for the compressible Navier-Stokes equations. Universitat Politècnica de Catalunya, Barcelona (2015)